

Blind Swarms for Coverage in 2-D

Vin de Silva
Department of Mathematics
Stanford University
Palo Alto, CA 94305 USA

Robert Ghrist
Department of Mathematics and
Coordinated Sciences Laboratory
University of Illinois
Urbana, IL 61801 USA

Abubakr Muhammad
Department of Electrical Engineering
Georgia Institute of Technology
Atlanta, GA 30332 USA

Abstract—We consider coverage problems in robot sensor networks with minimal sensing capabilities. In particular, we demonstrate that a “blind” swarm of robots with no localization and only a weak form of distance estimation can rigorously determine coverage in a bounded planar domain of unknown size and shape. The methods we introduce come from algebraic topology.

I. COVERAGE PROBLEMS

Many of the potential applications of robot swarms require information about coverage in a given domain. For example, using a swarm of robot sensors for surveillance and security applications carries with it the charge to maximize, or, preferably, guarantee coverage. Such applications include networks of security cameras, mine field sweeping via networked robots [18], and oceanographic sampling [4]. In these contexts, each robot has some coverage domain, and one wishes to know about the union of these coverage domains. Such problems are also crucial in applications not involving robots directly, e.g., communication networks.

As a preliminary analysis, we consider the static “field” coverage problem, in which robots are assumed stationary and the goal is to verify blanket coverage of a given domain. There is a large literature on this subject; see, e.g., [7], [1], [16]. In addition, there are variants on these problems involving “barrier” coverage to separate regions. Dynamic or “sweeping” coverage [3] is a common and challenging task with applications ranging from security to vacuuming. Although a sensor network composed of robots will have dynamic capabilities, we restrict attention in this brief paper to the static case in order to lay the groundwork for future inquiry.

There are two primary approaches to static coverage problems in the literature. The first uses computational geometry tools applied to exact node coordinates. This typically involves ‘ruler-and-compass’ style geometry [10] or Delaunay triangulations of the domain [16], [14], [20]. Such approaches are very rigid with regards to inputs: one must know exact node coordinates and one must know the geometry of the domain precisely to determine the Delaunay complex.

To alleviate the former requirement, many authors have turned to probabilistic tools. For example, in [13], the author assumes a randomly and uniformly distributed collection of nodes in a domain with a fixed geometry and proves expected

area coverage. Other approaches [15], [19] give percolation-type results about coverage and network integrity for randomly distributed nodes. The drawback of these methods is the need for strong assumptions about the exact shape of the domain, as well as the need for a uniform distribution of nodes.

In the sensor networks community, there is a compelling interest (and corresponding burgeoning literature) in determining properties of a network in which the nodes do not possess coordinate data. One example of a coordinate-free approach is in [17], which gives a heuristic method for geographic routing without coordinate data: among the large literature arising from this paper, we note in particular the mathematical analysis of this approach in [11]. To our knowledge, no one has treated the coverage problem in a coordinate-free setting.

In this note, we introduce a new set of tools for answering coverage problems in robotics and sensor networks with minimal assumptions about domain geometry and node localization. We provide a sufficiency criterion for coverage. We do not answer the problem of how the nodes should be placed in order to maximize coverage, nor the minimum number of such nodes necessary; neither do we address how to reallocate nodes to fill coverage holes.

A. Assumptions

The methods we introduce are meant to work in settings where there are a large number of robots which are relatively simple. They have very limited range and are devoid of localization and orientation capabilities, possessing merely a discrete form of distance measurement. More specifically, each node has a unique ID which it broadcasts. All other robots within range can “hear” its neighbor as either a strong or weak signal, depending on the distance to that node. This bimodal signal reading is not motivated by current hardware capabilities. Recent work by the authors [6] allows for more realistic sensor assumptions.

We work under the following assumptions:

- A1** Nodes have radially symmetric covering domains (for sensing or broadcasting) of **cover** radius r_c .
- A2** Nodes broadcast their unique ID numbers. Each robot can detect the identity of anyone within radius r_s via a **strong** signal, and via a **weak** signal within a larger radius r_w .
- A3** The radii of communication r_s, r_w and the covering

radius r_c satisfy

$$r_c \geq r_s \sqrt{\frac{1}{3}} \quad ; \quad r_w \geq r_s \sqrt{\frac{13}{3}}. \quad (1)$$

A4 Nodes lie in a bounded planar domain $\mathcal{D} \subset \mathbb{R}^2$. Nodes can detect the presence (but not the location or direction) of the boundary $\partial\mathcal{D}$ within a fixed **fence detection radius** $r_f \geq 0$.

A5 The restricted domain $\mathcal{D} - \mathcal{C}$ is connected, where \mathcal{C} denotes the collar

$$\mathcal{C} = \left\{ x \in \mathcal{D} : \|x - \partial\mathcal{D}\| \leq r_f + \frac{1}{2}r_s \right\}. \quad (2)$$

A6 The curve(s) $\{x \in \mathcal{D} : \|x - \partial\mathcal{D}\| = r_f\}$ have internal injectivity radius $\frac{1}{2}r_s$ and external injectivity radius $\min\{r_f + \frac{1}{2}r_s, r_s\}$.

Assumptions **A1-A4** specify the communication capabilities of the nodes. Assumption **A5** is needed to prevent the domain from being too ‘pinched’ (see Fig. 1[left]). This is clearly necessary since nodes with neither map nor coordinates cannot distinguish between a pinched domain and a disconnected domain. Assumption **A6** means that the outermost boundary cannot exhibit large-scale ‘wrinkling’ (see Fig. 1[right]). This assumption is used in the details of the proof of Theorem 3 for eliminating pathological configurations. See Remark 11 for discussion on weakening this condition.

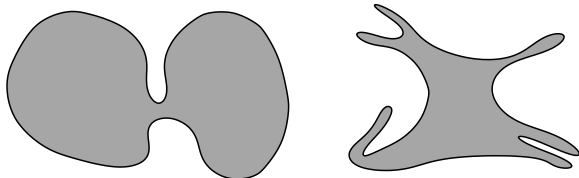


Fig. 1. Two types of illegal domains, violating **A5** and **A6**.

The last assumptions, **A5** and **A6**, are the only restrictions on the geometry of the domain. We emphasize that the number of boundary components is not assumed to be known: nodes have no information about the boundary other than whether they are within range r_f . This r_f is independent of the node-to-node communication radii r_s and r_w and the coverage radius r_c . The area of the domain is not assumed to be known, and convexity is not at all required.

B. Results

Surprisingly, such coarse coordinate-free data is sufficient to rigorously verify coverage in many instances. More specifically, we give coverage verification criteria for the restricted domain of points not too close to the boundary. Our results require a centralized computation. At this time, we do not solve the challenging problem of having the network of nodes perform local, asynchronous computations to determine coverage (as in, e.g., [3]).

Our strategy is as follows. We build a nested collection of graphs and corresponding simplicial complexes:

$$\begin{array}{ccc} G_s & \xrightarrow{\subset} & G_w \\ \cup \uparrow & & \cup \uparrow \\ F_s & \xrightarrow{\subset} & F_w \end{array} \quad \begin{array}{ccc} \mathcal{R}_s & \xrightarrow{\subset} & \mathcal{R}_w \\ \cup \uparrow & & \cup \uparrow \\ \mathcal{F}_s & \xrightarrow{\subset} & \mathcal{F}_w \end{array} \quad (3)$$

The graphs G_s and G_w are determined as follows: the vertices are \mathcal{X} , the nodes of the network, and the edges are present between nodes which are within distance r_s and r_w respectively. These are **communication graphs** for the strong and weak signals respectively. The graphs F_s and F_w are the strong and weak **fence subgraphs** — the maximal subgraphs of G_s (respectively G_w) whose nodes all lie within the fence detection radius. These graphs are ‘filled in’ to yield the corresponding simplicial complexes. (Each is the largest simplicial complex with the corresponding graph as its 1-d skeleton.)

The **sensor cover**, \mathcal{U} , is the union over \mathcal{X} of discs of radius r_c . Our results on the coverage of \mathcal{U} are all based on **homology**: an algebraic topological invariant of these simplicial complexes (see Section II-B). The following is the principal criterion for coverage we derive in this paper.

Main Theorem: *For a system satisfying **A1-A6**, the region $\mathcal{D} - \mathcal{C}$ is contained in the sensor cover \mathcal{U} if there is a homology class in $H_2(\mathcal{R}_s, \mathcal{F}_s)$ which is nonzero in $H_2(\mathcal{R}_w, \mathcal{F}_w)$.*

II. TOPOLOGICAL TOOLS

We begin with two constructions for transforming network data into topological spaces. Though these constructions are classical in topology, they appear to be unused in sensor networks problems. For reasons of space constraints, we give a sparse primer: see [8], [12] for a complete introduction.

A. Complexes and communication

The problem of computing the topological type of a union of sets is classical, and easily handled using the concept of a Čech complex.

Definition 1: Given a collection of sets $\mathcal{U} = \{U_\alpha\}$, the **Čech complex** of \mathcal{U} , $\check{C}(\mathcal{U})$, is the abstract simplicial complex whose k -simplices correspond to nonempty intersections of $k + 1$ distinct elements of \mathcal{U} .

The **Čech Theorem** states that for sufficiently well-behaved sets U_α (convex will suffice), the union $\cup_\alpha U_\alpha$ has the same topological type as the Čech complex \check{C} . By ‘topological type’ we mean homotopy equivalence. See, e.g., [2] for definitions and a proof.

Unfortunately, it is highly nontrivial to compute a Čech complex: one needs very precise data on robot locations, since small perturbations can change the overlap regions. In the context of a ‘blind’ swarm of robots, the Čech complex is seemingly unattainable. Therefore, we consider the following related construction, which is more adapted to communication network constraints.

Definition 2: Given a set of points $\mathcal{X} = \{x_\alpha\} \subset \mathbb{R}^n$ in Euclidean n -space and a fixed radius ϵ , the **Rips complex** of \mathcal{X} , $\mathcal{R}(\mathcal{X})$, is the abstract simplicial complex whose k -simplices correspond to unordered $(k+1)$ -tuples of points in \mathcal{X} which are pairwise within Euclidean distance ϵ of each other.

The Rips complex is ideally suited to communication networks, since the entire complex is determined by pairwise communication data. Unfortunately, the Rips complex does not necessarily capture the topology of the union of cover discs: we have traded computability for accuracy. Figure 2 gives a fundamental class of examples for which the Rips complex fails to capture the Čech complex.

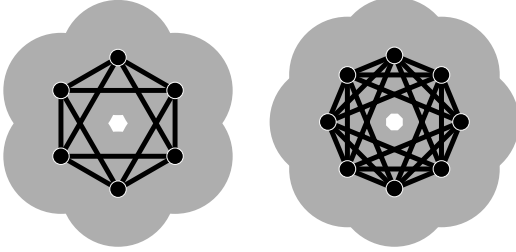


Fig. 2. A class of examples for which the Rips complex \mathcal{R}_s detects ‘phantom’ topological features. Take $2k+2$ points equidistributed on a circle of diameter $r_s + \epsilon$ where $\epsilon \ll 1$. The Čech complex is homotopy equivalent to a circle, as the Čech Theorem requires. The Rips complex however is isomorphic to the boundary of a *cross-polytope* in $k+1$ dimensions. This Rips complex is thus homeomorphic to the sphere S^k and accordingly is very different from the Čech complex for $k > 1$. [left] $k = 2$, with \mathcal{R}_s an octahedron. [right] $k = 3$.

B. Simplicial homology

Homology is an algebraic procedure for counting various types of holes in a space. We briefly describe **simplicial homology with real coefficients**: see [8], [12] for comprehensive introductions.

Let X denote an n -dimensional simplicial complex. Roughly speaking, the homology of X , denoted $H_*(X)$, is a sequence of vector spaces $\{H_k(X) : k = 0, 1, 2, 3, \dots\}$, where $H_k(X)$ is called the **k -dimensional homology of X** . The dimension of $H_k(X)$, called the k^{th} **Betti number of X** , is a coarse measurement of the number of different holes in the space X that can be sensed by using subcomplexes of dimension k . For us, $H_1(X)$ and $H_2(X)$ will be most important. A generator for $H_1(X)$ consists of a set of edges in X forming an oriented loop. A generator for $H_2(X)$ consists of 2-simplices which form an oriented simplicial surface without boundary.

Let X denote a simplicial complex. Define for each $k \geq 0$, the vector space $C_k(X)$ to be the vector space whose basis is the set of **oriented** k -simplices of X ; that is, a k -simplex $\{v_0, \dots, v_k\}$ together with an order type denoted $[v_0, \dots, v_k]$ where a change in orientation corresponds to a change in the sign of the coefficient:

$$[v_0, \dots, v_i, \dots, v_j, \dots, v_k] = -[v_0, \dots, v_j, \dots, v_i, \dots, v_k]. \quad (4)$$

For k larger than the dimension of X , $C_k(X) = 0$. The **boundary map** is defined to be the linear transformations $\partial : C_k \rightarrow C_{k-1}$ which acts on basis elements $[v_0, \dots, v_k]$ via

$$\partial[v_0, \dots, v_k] := \sum_{i=0}^k (-1)^i [v_0, \dots, v_{i-1}, v_{i+1}, \dots, v_k]. \quad (5)$$

This gives rise to a **chain complex**: a sequence of vector spaces and linear transformations

$$\dots \xrightarrow{\partial} C_{k+1} \xrightarrow{\partial} C_k \xrightarrow{\partial} C_{k-1} \dots \xrightarrow{\partial} C_1 \xrightarrow{\partial} C_0 \quad (6)$$

Consider the following two subspaces of C_k : the **cycles** (those subcomplexes without boundary) and the **boundaries** (those subcomplexes which are themselves boundaries).

$$\begin{aligned} k\text{-cycles} & : Z_k(X) = \ker(\partial : C_k \rightarrow C_{k-1}) \\ k\text{-boundaries} & : B_k(X) = \text{im}(\partial : C_{k+1} \rightarrow C_k) \end{aligned} \quad (7)$$

A simple lemma demonstrates that $\partial \circ \partial = 0$; that is, the boundary of a chain has empty boundary. It follows that B_k is a subspace of Z_k . The k -cycles in X are the basic objects which count the presence of a ‘hole of dimension k ’ in X . But, certainly, many of the k -cycles in X are measuring the same hole; still other cycles do not really detect a hole at all — they bound a subcomplex of dimension $k+1$ in X .

We say that two cycles ξ and η in $Z_k(X)$ are **homologous** if their difference is a boundary:

$$[\xi] = [\eta] \iff \xi - \eta \in B_k(X). \quad (8)$$

The k -dimensional **homology** of X , denoted $H_k(X)$ is the quotient vector space,

$$H_k(X) = \frac{Z_k(X)}{B_k(X)}. \quad (9)$$

Specifically, an element of $H_k(X)$ is an equivalence class of homologous k -cycles. This inherits the structure of a vector space in the natural way: $[\xi] + [\eta] = [\xi + \eta]$ and $c[\xi] = [c\xi]$ for $c \in \mathbb{R}$.

The precise version of homology used in our theorems is a ‘relative’ homology. Often, one wishes to compute holes modulo some region of the space. Let $Y \subset X$ be a subcomplex of X . We define the **relative chains** as follows: $C_k(X, Y)$ is the quotient space obtained from $C_k(X)$ by collapsing the subspace generated by k -simplices in Y . One verifies that this quotient is respected by ∂ and that the subspaces defined by the kernel and image are well-defined and satisfy

$$B_k(X, Y) \subset Z_k(X, Y) \subset C_k(X, Y). \quad (10)$$

It then follows that the **relative homology**

$$H_k(X, Y) = \frac{Z_k(X, Y)}{B_k(X, Y)} \quad (11)$$

is well-defined. This homology $H_*(X, Y)$ measures holes detected by chains whose boundaries lie in Y .

Consider two simplicial complexes X and X' . Let $f : X \rightarrow X'$ be a continuous simplicial map: f takes each k -simplex of X to a k' -simplex of X' , where $k' \leq k$. Then, the map f

induces a linear transformation $f_{\#} : C_k(X) \rightarrow C_k(X')$. It is a simple lemma to show that $f_{\#}$ takes cycles to cycles and boundaries to boundaries; hence there is a well-defined linear transformation on the quotient spaces

$$f_* : H_k(X) \rightarrow H_k(X') \quad : \quad f_* : [\xi] \mapsto [f_{\#}(\xi)]. \quad (12)$$

This is called the **induced homomorphism** of f . Functoriality implies that (1) the identity map $Id : X \rightarrow X$ induces the identity map on homology; and (2) the composition of two maps $g \circ f$ induces the composition of the linear transformation: $(g \circ f)_* = g_* \circ f_*$.

III. A HOMOLOGICAL CRITERION

We present and prove a criterion for coverage based on the inclusion map $\iota : (\mathcal{R}_s, \mathcal{F}_s) \hookrightarrow (\mathcal{R}_w, \mathcal{F}_w)$.

Theorem 3: For a fixed set of robots \mathcal{X} in a domain $\mathcal{D} \subset \mathbb{R}^2$ satisfying assumptions **A1-A6**, the sensor cover \mathcal{U} contains $\mathcal{D} - \mathcal{C}$ if the induced homomorphism

$$\iota_* : H_2(\mathcal{R}_s, \mathcal{F}_s) \rightarrow H_2(\mathcal{R}_w, \mathcal{F}_w) \quad (13)$$

is nonzero.

A. Intuition and persistence

It is a fact that, under assumption **A5**, the relative homology $H_2(\mathcal{D}, \mathcal{C})$ has dimension exactly 1. Furthermore, it is true that if \mathcal{U} is the union of the cover discs, then $H_2(\mathcal{U} \cup \mathcal{C}, \mathcal{C})$ is nonzero if and only if \mathcal{U} contains $\mathcal{D} - \mathcal{C}$.

However, we cannot compute \mathcal{U} directly. As mentioned in Section II-A, the simplicial complex which captures the topology of \mathcal{U} — the Čech complex — is hard to compute, even with a global coordinate system. Rips complexes are, in contrast, very manageable with merely communication data (and hence computable on the hardware level). Thus, it would make sense to hope that if $H_2(\mathcal{R}_s, \mathcal{F}_s)$ is nonzero, then $\mathcal{U} \subset \mathcal{D} - \mathcal{C}$. Indeed, these two events coincide for systems like those illustrated in Figs. 4-5.

But this is not always the case. Consider the setting of Fig. 3, in which there is a cycle of points within \mathcal{F}_s all of which are attached to a single vertex in $\mathcal{R}_s - \mathcal{F}_s$. This cycle is such that two of the edges are of length r_s , while the other two edges are of length $\epsilon \ll r_s$. As such, neither of the diagonals is of length r_s and is therefore not present in \mathcal{F}_s . This system has $H_2(\mathcal{R}_s, \mathcal{F}_s) \neq 0$: there exist “fake” relative 2-cycles which do not imply coverage of the entire domain. Other fake relative 2-cycles can be generated from the examples of Fig. 2.

Note, however, what happens to this relative 2-cycle under increasing the communication radius from r_s to r_w , then the loop in \mathcal{F}_s is “filled in” by diagonals, and the image of this fake class under ι_* is the zero element of $H_2(\mathcal{R}_w, \mathcal{F}_w)$. Assuming that these points are a portion of a larger subset of nodes, it is *not necessarily* the case that $H_2(\mathcal{R}_w, \mathcal{F}_w) = 0$, since there may be a new fake 2-cycle which comes into existence at the longer communication lengths: but the original fake 2-cycle is annihilated by ι_* .

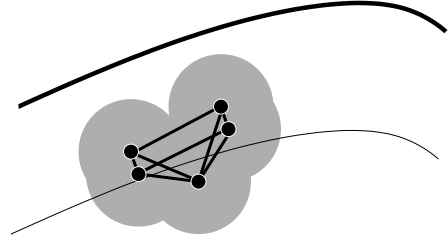


Fig. 3. A fake generator for $H_2(\mathcal{R}_s, \mathcal{F}_s)$ which is annihilated by inclusion ι_* into $H_2(\mathcal{R}_w, \mathcal{F}_w)$. The strip illustrated is a collar of radius r_f .

B. Preliminary lemmas

The following result tells us that the Čech complex can be “squeezed” between two Rips complexes of different radii.

Lemma 4: Let \mathcal{X} be a set of points in \mathbb{R}^2 and $\check{C}_\epsilon(\mathcal{X})$ the Čech complex of the cover of \mathcal{X} by balls of radius $\epsilon/2$. Then there is sequence of inclusions

$$\mathcal{R}_{\epsilon'}(\mathcal{X}) \subset \check{C}_\epsilon(\mathcal{X}) \subset \mathcal{R}_\epsilon(\mathcal{X}) \quad \text{whenever} \quad \frac{\epsilon}{\epsilon'} \geq \frac{2}{\sqrt{3}}. \quad (14)$$

Moreover, this ratio is the smallest for which the inclusions hold in general.

Proof: The second inclusion is trivial because the criterion for inclusion of a simplex in \mathcal{R}_ϵ is weaker than the criterion for inclusion of a simplex in \check{C}_ϵ . The first inclusion is equivalent to the following assertion: if a collection of points in \mathbb{R}^2 is such that every pair is separated by a distance at most ϵ' , then the balls of radius $\epsilon/2$ centered on these points have a common intersection.

It suffices to prove this for a triple of points thanks to Helly’s theorem [9], which implies that a collection of $k \geq 4$ convex sets in \mathbb{R}^2 has a nonempty common intersection provided only that the same is true for each subset of size 3. If we have k points spanning a simplex in $\mathcal{R}_{\epsilon'}$, and if we show that each triple of the $\epsilon/2$ -balls at these vertices must have a nonempty intersection, then, by Helly’s theorem, the same is true for the entire set of k balls. Hence the vertices span a simplex in \check{C}_ϵ .

Therefore, consider a triple of points a, b, c which span a triangle with side lengths at most ϵ' . We must show that the three discs of radius $\epsilon/2$ centered on a, b, c meet at a common point. If the triangle is obtuse (or right-angled), then the midpoint of the longest side is common to all three discs. Indeed, this is even true with radius $\epsilon'/2$. If the triangle is acute then the largest angle, say A at vertex a , satisfies $\pi/3 \leq A \leq \pi/2$ and so $\sin(A) \geq \sqrt{3}/2$. We can compute the circumradius R of the triangle abc as $R = |bc|/2 \sin A$ and hence we deduce $R \leq \epsilon'/\sqrt{3} \leq \epsilon/2$. Thus, in this case, the three discs meet at the circumcenter.

To see that this ratio is optimal, consider an equilateral triangle of side length ϵ' . \diamond

Lemma 5: For any collection of nodes in \mathcal{D} which form a simplex of \mathcal{R}_s , its convex hull lies within \mathcal{U} for r_c satisfying **A3**.

Proof: This follows from the proof of Lemma 4 and the fact that a collection of circular disks which meet at a common point x necessarily covers the convex hull of x and the centers of the discs. \diamond

Remark 6: It follows from Lemma 5 that Theorem 3 is true in the trivial situation where $\mathcal{D} - \mathcal{C}$ is entirely contained inside some triangle of \mathcal{R}_s . We assume henceforth that our configuration does not degenerate in this sense.

Lemma 7: Let $\bar{\mathcal{C}} := \mathbb{R}^2 - (\mathcal{D} - \mathcal{C})$ denote the **extended collar** of \mathcal{D} . For any collection of nodes in \mathcal{D} which form a simplex of \mathcal{F}_s , its convex hull lies within $\bar{\mathcal{C}}$.

Proof: It suffices, by Carathéodory's Theorem [9], to show that the triangles of \mathcal{F}_s lie within $\bar{\mathcal{C}}$. In fact, since $\mathcal{D} - \mathcal{C} = \mathcal{D} - \bar{\mathcal{C}}$ is connected and since we have ruled out the situation of Remark 6, it suffices to consider edges. For any point p on an edge in \mathcal{F}_s , the distance from p to a vertex in \mathcal{F}_s is bounded by $r_s/2$. The triangle inequality completes the proof. \diamond

The last and most technical lemma is a variant of Lemma 4 adapted to a cycle in an annular region of thickness Δ . By this we mean a domain homeomorphic to $S^1 \times [0, 1]$ which can be foliated by line segments of length no more than Δ .

Lemma 8: Assume an annular region \mathcal{S} in \mathbb{R}^2 of thickness Δ and a collection of points $\mathcal{X} \subset \mathcal{S}$ which forms a 1-cycle $[\gamma] \in H_1(\mathcal{R}_{\epsilon'}(\mathcal{X}))$, where γ is contained entirely within \mathcal{S} . If $[\gamma] = 0$ in $H_1(\mathcal{S})$, then it is also trivial in the ϵ' Rips complex $\mathcal{R}_{\epsilon'}(\mathcal{X})$, where

$$\epsilon' = \sqrt{\epsilon^2 + \Delta^2}. \quad (15)$$

Proof: Denote by γ the cycle as a 1-d loop in \mathcal{S} and let U' denote the union over \mathcal{X} of discs of radius $\epsilon'/2$. Note that by our choice of ϵ' , U' contains the set \mathcal{U} obtained by covering every point of γ (edges as well as vertices) with a ball of radius $\Delta/2$.

Assume by way of contradiction that $[\gamma] \neq 0$ in $H_1(\mathcal{R}_{\epsilon'}(\mathcal{X}))$ yet is trivial in $H_1(\mathcal{S})$. From Lemma 4, $\mathcal{R}_{\epsilon'}(\mathcal{X}) \subseteq \check{C}_{\epsilon'}(\mathcal{X}) \subseteq \mathcal{R}_{\epsilon'}(\mathcal{X})$. Thus, γ is a nontrivial loop in $\check{C}_{\epsilon'}(\mathcal{X})$. By the Čech Theorem and Alexander duality, there exists a point $p \in \mathcal{S} - U'$ enclosed by γ .

Since \mathcal{S} has thickness Δ , there is a line segment ℓ in \mathcal{S} of length Δ passing through p and connecting the two boundary components of \mathcal{S} . As γ is trivial in $H_1(\mathcal{S})$, ℓ must intersect γ in at least two points; thus, since ℓ passes through p , ℓ intersects U' in at least two disjoint segments. Each such segment must have length at least $\Delta/2$: contradiction. \diamond

C. Proof of Theorem 3

Proof: We consider the simplicial realization map $\sigma : \mathcal{R}_s \rightarrow \mathbb{R}^2$ which sends vertices of \mathcal{R}_s to the points $\mathcal{X} \subset \mathcal{D}$ and which sends a k -simplex of \mathcal{R}_s to the (potentially singular) k -simplex given by the convex hull of the vertices implicated. From Lemma 7, σ takes the pair $(\mathcal{R}_s, \mathcal{F}_s)$ to $(\mathbb{R}^2, \bar{\mathcal{C}})$; we

therefore construct the following diagram:

$$\begin{array}{ccc} H_2(\mathcal{R}_s, \mathcal{F}_s) & \xrightarrow{\delta_*} & H_1(\mathcal{F}_s) \\ \downarrow \sigma_* & & \downarrow \sigma_* \\ H_2(\mathbb{R}^2, \bar{\mathcal{C}}) & \xrightarrow{\delta_*} & H_1(\bar{\mathcal{C}}) \end{array} \quad (16)$$

Here, δ_* acts on a class $[\alpha] \in H_2(\mathcal{R}_s, \mathcal{F}_s)$ by taking the boundary: $\delta_*[\alpha] = [\partial\alpha] \in H_1(\mathcal{F}_s)$. The diagram of Eqn. (16) is commutative: $\delta_*\sigma_* = \sigma_*\delta_*$. The homology class $\sigma_*\delta_*[\alpha]$ measures how many times the boundary of α “wraps around” the extended collar $\bar{\mathcal{C}}$.

Case 1: $\sigma_*\delta_*[\alpha] \neq 0$.

By commutativity of Eqn. (16), $\delta_*\sigma_*[\alpha] = \sigma_*\delta_*[\alpha] \neq 0$. Hence, $\sigma_*[\alpha] \neq 0$. Assume that \mathcal{U} does not contain $\mathcal{D} - \mathcal{C}$ and choose $p \in \mathcal{D} - (\mathcal{C} \cup \mathcal{U})$. Since, by Lemma 5, every point in $\sigma(\mathcal{R}_s)$ lies within \mathcal{U} , this implies that $\sigma : (\mathcal{R}_s, \mathcal{F}_s) \rightarrow (\mathbb{R}^2, \bar{\mathcal{C}})$ factors through the pair $(\mathbb{R}^2 - p, \bar{\mathcal{C}})$. However, $H_2(\mathbb{R}^2 - p, \bar{\mathcal{C}}) = 0$ since, by Alexander duality, $H_2(\mathbb{R}^2 - p, \bar{\mathcal{C}}) = H^0(\mathbb{R}^2 - \bar{\mathcal{C}}, p)$, which vanishes since $\mathbb{R}^2 - \bar{\mathcal{C}}$ is connected. Thus, $\sigma_*[\alpha] = 0$: contradiction.

Case 2: $\sigma_*\delta_*[\alpha] = 0$.

We demonstrate that this case is impossible under the hypothesis $\iota_*[\alpha] \neq 0$. We construct the following commutative diagram with three rows, the top and bottom of which come from the **long exact sequence** [8] of the pairs $(\mathcal{R}_s, \mathcal{F}_s)$ and $(\mathcal{R}_w, \mathcal{F}_w)$ respectively. The middle row comes from the pair $(\mathcal{R}_m, \mathcal{F}_m)$ — the Rips and Fence complexes computed at the “midrange” signal of radius $r_m = r_s\sqrt{13}/2$. The inclusion map $\iota : (\mathcal{R}_s, \mathcal{F}_s) \hookrightarrow (\mathcal{R}_w, \mathcal{F}_w)$ factors through the pair $(\mathcal{R}_m, \mathcal{F}_m)$.

$$\begin{array}{ccccc} H_2(\mathcal{R}_s) & \xrightarrow{j_*} & H_2(\mathcal{R}_s, \mathcal{F}_s) & \xrightarrow{\delta_*} & H_1(\mathcal{F}_s) \\ \downarrow \iota_* & & \downarrow \iota_* & & \downarrow \iota_* \\ H_2(\mathcal{R}_m) & \xrightarrow{j_*} & H_2(\mathcal{R}_m, \mathcal{F}_m) & \xrightarrow{\delta_*} & H_1(\mathcal{F}_m) \\ \downarrow \iota_* & & \downarrow \iota_* & & \downarrow \iota_* \\ H_2(\mathcal{R}_w) & \xrightarrow{j_*} & H_2(\mathcal{R}_w, \mathcal{F}_w) & \xrightarrow{\delta_*} & H_1(\mathcal{F}_w) \end{array} \quad (17)$$

Here, j_* is the map induced by the projection chain map $j : C_2(\mathcal{R}) \rightarrow C_2(\mathcal{R}, \mathcal{F})$, and δ_* is as in Eqn. (16). The horizontal rows are **exact**, meaning that the kernel of δ_* is equal to the image of j_* .

We claim that there exists a representative $\alpha' \in [\alpha]$ such that the geometric 1-cycle $\sigma(\partial\alpha')$ is contained in a particular annular shell \mathcal{S} , defined as follows. Let κ denote the curves $\{x \in \mathcal{D} : \|x - \partial\mathcal{D}\| = r_f\}$, and let \mathcal{S} denote the set of points in \mathbb{R}^2 of distance $\frac{1}{2}r_s$ from κ in the interior region and within distance $\min\{r_f + \frac{1}{2}r_s, r_s\}$ of κ in the exterior of the region.

To determine α' , remove all triangles in α which are contained in \mathcal{F}_s to get a new cycle. This represents the same class in relative homology, and, moreover, every edge of $\partial\alpha'$ is the face of a triangle with a vertex in $\mathcal{R}_s - \mathcal{F}_s$. It follows that all edges of the 1-cycle $\partial\alpha'$ must lie within \mathcal{S} using arguments as in Lemma 7.

From **A6**, we know that \mathcal{S} is a disjoint collection of annular regions each of thickness at most $\frac{3}{2}r_s$. Since $\sigma_*\delta_*[\alpha] = 0$, we know that the 1-cycle $\partial\alpha'$ is nullhomologous within \mathcal{S} . Apply Lemma 8 with $\epsilon = r_s$, $\Delta = 3r_s/2$, and $\epsilon' = r_s\sqrt{13}/2$ to conclude that by increasing the radius from r_s to r_m , the cycle $\partial\alpha'$ becomes trivial: hence, $\iota_*\delta_*[\alpha] = 0 \in H_1(\mathcal{F}_m)$.

We may now rule out Case 2 as follows. By hypothesis, $[\alpha] \in H_2(\mathcal{R}_s, \mathcal{F}_s)$ is nonzero, as is $\iota_*\iota_*[\alpha] \in H_2(\mathcal{R}_w, \mathcal{F}_w)$. In the present case, $\iota_*\delta_*[\alpha] = 0$ in $H_1(\mathcal{F}_m)$. Commutativity of Eqn. (17) implies that $\delta_*\iota_*[\alpha] = 0$. By exactness of this row, $\iota_*[\alpha] = j_*[\zeta]$ for some $[\zeta] \in H_2(\mathcal{R}_m)$. An application of Lemma 4 implies that the map $\iota_* : H_2(\mathcal{R}_m) \rightarrow H_2(\mathcal{R}_w)$ factors through the homology of the Čech complex $\check{C}_w = \check{C}_w(\mathcal{X})$ of the cover of \mathcal{X} with balls of radius $r_w/2$:

$$\iota_* : H_2(\mathcal{R}_m) \rightarrow H_2(\check{C}_w) \rightarrow H_2(\mathcal{R}_w). \quad (18)$$

From the Čech Theorem, \check{C}_w has the homotopy type of a subset of \mathbb{R}^2 . Any such subset has no homology in dimension 2; hence $H_2(\check{C}_w) = 0$. We conclude that $\iota_*[\zeta] = 0$. It follows from commutativity of Eqn. (17) that

$$0 = j_*(\iota_*[\zeta]) = \iota_*(j_*[\zeta]) = \iota_*(\iota_*[\alpha]) \neq 0. \quad (19)$$

Contradiction. Case 2 is impossible under the assumption that $r_w \geq r_s(\sqrt{13}/2)(2/\sqrt{3})$, which agrees with **A3**. \diamond

IV. SIMULATIONS

The past five years has witnessed the creation of several algorithms for quickly computing homology of complexes (see [5], [12], [21] and works cited there). In order to demonstrate the homological criterion, we have successfully run several simulations using the computational homology software packages `Plex` [23]. `Plex` computes dimensions of persistent homology groups.

Simulations for both packages have been written using MATLAB as the frontend (primarily for generating the simplicial complexes from various point-data sets, data formatting and for visualization.) The `Plex` package has been used for computing homology. We note also the utility of an alternate homology software package, `CHomP` [22], which returns explicit generators, and hence gives more precise information than `Plex`, at the cost of running much more slowly. The current implementation of `Plex` computes only the dimensions of persistent homology groups (see, e.g., [21]), which is enough to check whether the homomorphism ι_* in the criterion of Theorem 3 is nonvanishing.

Remark 9: In order to compute homology relative to the fence subcomplexes, we use the following procedure. To compute $H_2(\mathcal{R}_s, \mathcal{F}_s)$, we begin by adding an abstract vertex to \mathcal{R}_s and then augmenting this vertex to every simplex in \mathcal{F}_s . This is called placing a **cone** over \mathcal{F}_s , and it yields a complex $\mathcal{Q}(\mathcal{R}_s, \mathcal{F}_s)$ whose homotopy type is that of the

quotient space $\mathcal{R}_s/\mathcal{F}_s$. It follows from the Excision Theorem [8] and homotopy invariance that

$$H_*(\mathcal{R}_s, \mathcal{F}_s) \cong H_*(\mathcal{R}_s/\mathcal{F}_s) \cong H_*(\mathcal{Q}(\mathcal{R}_s, \mathcal{F}_s)), \quad (20)$$

hence, this construction faithfully captures the homology.

Remark 10: To avoid round-off error in homology computations, we use homology with coefficients in \mathbb{Z}_2 . All of our arguments are independent of the field coefficients used; hence the criterion is still valid with this assumption.

Remark 11: The precise statement of **A6** in terms of injectivity radii requires the curve to be smooth. From the proof of Theorem 3, it is clear that the crucial condition is to have the shell \mathcal{S} represent annular domains of thickness bounded by $\frac{3}{2}r_s$. In practice, having \mathcal{D} piecewise-linear is admissible: even though the injectivity radii degenerate to zero, the set \mathcal{S} is still an annular region(s) of width bounded by some larger length, depending on the sharpness of the curves. For a piecewise-linear $\partial\mathcal{D}$, an increase in r_w based on the angle of the sharpest corner in the outermost boundary component makes the criterion rigorous.

Note that in the figures and examples which follow, we illustrate the cover using coordinates. The frontend keeps track of coordinates for purposes of drawing pictures. However, `Plex` receives no information about coordinates: the homology criterion uses *only* connectivity data as per our assumptions.

Examples of successful applications of the homological criterion of Theorem 3 appear in Figures 4 and 5. The first of these domains is simply-connected, the second is not. In both instances the data is presented as embedded in the domain \mathcal{D} and the cover \mathcal{U} is illustrated. In neither case is the cover too redundant — there are regions which are covered by only one node. Simulations were run on a Linux/PC 1-Gbyte Memory Dual Processor Intel Xeon CPU 1700MHz; cache size 256 KB; MATLAB ver 6.5. The run time for `Plex` to compute the existence of a nontrivial persistent homology generator is roughly 7 seconds and 16 seconds for the systems of Figs. 4 and 5 respectively. The vast majority of the run time is spent constructing the simplicial complexes from the input data: the actual persistence computation is much faster. The system of Fig. 5 is the more complex of the two, having 172 nodes and a total of 135295 3-d simplices in \mathcal{R}_w .

V. CONCLUSIONS

The coverage criterion presented here is unique in its use of ideas and methods from homology theory: this represents the first application of homology theory to sensor networks problems. It is also unique in the minimal amount of knowledge of the environment required to guarantee coverage. We are aware of no other results that can guarantee coverage without information about either node coordinates or domain size/topology.

There are however several drawbacks to the criterion as here presented:

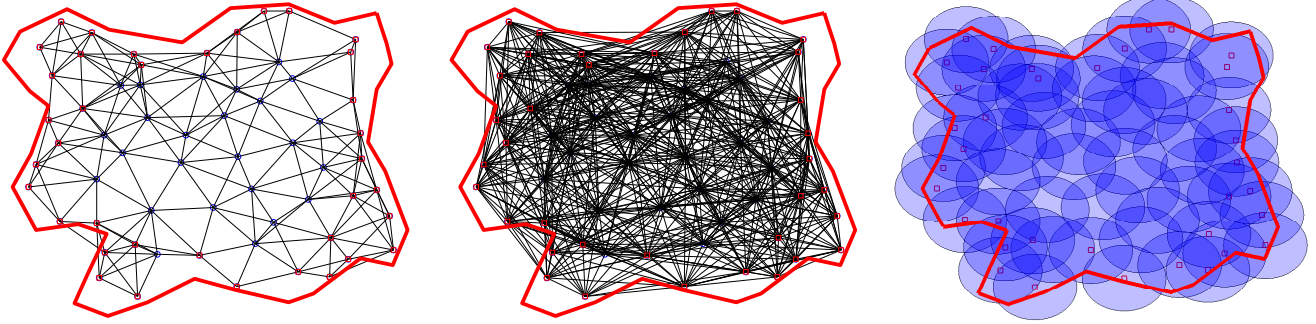


Fig. 4. An example of a system of 60 nodes in a simply-connected domain for which the homological criterion holds: [left] \mathcal{R}_s , [center] \mathcal{R}_w , [right] \mathcal{U} .

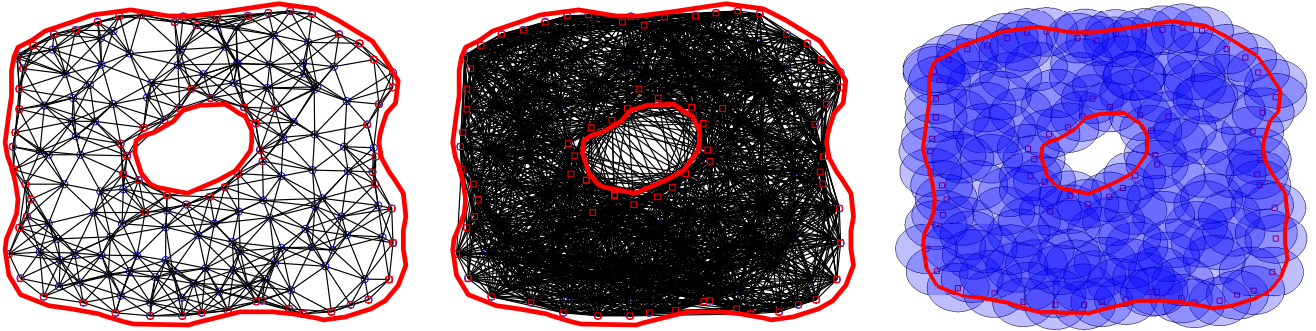


Fig. 5. An example of a system of 172 nodes in a domain with multiple boundary components for which the homological criterion is satisfied: [left] \mathcal{R}_s , [center] \mathcal{R}_w , [right] \mathcal{U} .

- 1) The criterion is not if-and-only-if and, indeed, works only when r_w and r_f are not too large with respect to the size of the domain. Figure 6 shows an example of a cover for which the homology criterion fails for several reasons. There are not enough points near the boundary to get a relative homology class. As well, there is a region of ‘fragile’ coverage which corresponds to a nontrivial 1-cycle in \mathcal{R}_s with four edges.
- 2) The criterion requires a centralized computation of a potentially large complexity. The input to the problem (the communication graphs) may be of size quadratic in the number of robots. Current homology algorithms are provably subquadratic in the size of the input complex only for special classes of spaces [5].
- 3) The need for a dual-ranged signal sensing device (r_s versus r_w) is not necessarily concordant with current technology. A recent improvement in our methods [6] allows for a homological coverage criterion with a single communication radius, so long as the nodes on the boundary of the domain are appropriately controlled.
- 4) Bounds on r_w in **A3** require knowing something about injectivity radii. It would be preferable to have a criterion that works with no restriction on $\partial\mathcal{D}$ apart from, say, a lack of pinching.
- 5) If the coverage criterion fails, it is important to have a means of rigorously proving the existence and locations of holes.

A. Extensions and future work

The result of this paper is our initial exploration of homological methods for coverage. Archival publications stemming from this work will include the following:

- 1) The coverage criterion works for nodes in any dimension workspace. The constants in **A3**, **A5** and **A6** change as a function of dimension d , and the criterion requires a persistent homology class in $H_d(\mathcal{R}_s, \mathcal{F}_s)$; otherwise, the techniques are nearly identical.
- 2) By minimizing the persistent generator in its homology class $H_2(\mathcal{R}_s, \mathcal{F}_s)$, one determines which robots may be ‘‘turned off’’ or redeployed without sacrificing coverage.
- 3) Verifying multiple coverage (in, e.g., beacon navigation) is possible via a modification of constants in **A3**.
- 4) Time-dependent systems which have a sequence of updates to the communication graphs are amenable to homological methods. In particular, there exists a homological criterion for guaranteeing that no evader can avoid being in the cover for all time, even if the system never enjoys coverage at a fixed time step.

B. On the utility of blind swarms

The promise of utilizing large swarms of small-scale autonomous robots carries with it the challenge of dealing with fewer and weaker sensing capabilities. Our thesis is that very basic robots with only the ability to listen to neighbor identification signals — a blind swarm — can effectively solve

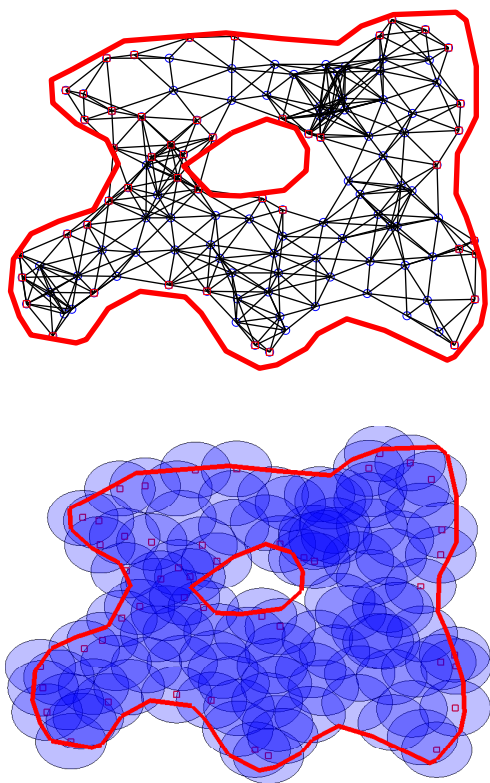


Fig. 6. An example of a system for which the homology criterion gives a false negative (the system covers the domain inside a neighborhood of the boundary). Note the fragility of the cover in the upper left portion, as is suggested by the quadrilateral 1-cycle in \mathcal{R}_s .

global problems. Coverage is one such problem, but is itself a prelude to further capabilities.

For example, consider a situation in which a system and domain satisfying **A1-A6** contains an unknown number of isolated objects of unknown shape and size on the floor. Assume further that the “wall detection” sensors of **A4** can distinguish whether the nearby wall is the boundary of the domain or if it is near one of the objects to be counted. It is possible to verify the exact number of objects with a “blind swarm” of robots with the limited capabilities envisioned in this paper. We outline the procedure.

- 1) Release a blind swarm in the domain \mathcal{D} and let them move according to a nearest-neighbor repulsion or by random diffusion. After a sufficient time, record pairwise communication data.
- 2) Compute the Rips complex \mathcal{R}_s and the fence subcomplex \mathcal{F}_s of nodes that detect either a wall or an object.
- 3) Compute the coverage criterion $\iota_* : H_2(\mathcal{R}_s, \mathcal{F}_s) \rightarrow H_2(\mathcal{R}_w, \mathcal{F}_w)$. If this vanishes, remix the swarm and recompute.
- 4) Let $\mathcal{O} \subset \mathcal{F}_s$ be the subcomplex generated by nodes which detect the objects.
- 5) *Proposition:* The number of objects in \mathcal{D} is equal to the dimension of $H_0(\mathcal{O})$.

We anticipate that topological tools will lead to more global capabilities for swarms of simple devices.

ACKNOWLEDGMENT

This work supported by DARPA # HR0011-05-1-0008 [RG], NSF PECASE Grant # DMS - 0337713 [RG], and EHS NSF-01-161 Grant # 0207411 [AM].

REFERENCES

- [1] M. A. Batalin and G. S. Sukhatme, “Spreading out: A local approach to multi-robot coverage,” in *Proc. of 6th International Symposium on Distributed Autonomous Robotic Systems*, (Fukuoka, Japan), 2002.
- [2] R. Bott and L. Tu, *Differential Forms in Algebraic Topology* Springer-Verlag, Berlin, 1982.
- [3] J. Cortés, S. Martínez, T. Karatas, and F. Bullo, “Coverage control for mobile sensing networks,” *IEEE Trans. Robotics. and Automation*, 20:2, pp. 243-255, 2004.
- [4] T. B. Curtin, J. G. Bellingham, J. Catipovic, and D. Webb, “Autonomous oceanographic sampling networks,” *Oceanography*, vol. 6, no. 3, pp. 86-94, 1993.
- [5] C. Delfinado and H. Edelsbrunner, “An incremental algorithms for Betti numbers of simplicial complexes on the 3-spheres,” *Comp. Aided Geom. Design*, 12:7, pp. 771-784, 1995.
- [6] V. de Silva and R. Ghrist, “Coordinate-free coverage in sensor networks with controlled boundaries,” in preparation.
- [7] D. W. Gage, “Command control for many-robot systems,” in *Nineteenth Annual AUVS Technical Symposium*, pp. 22-24, (Huntsville, Alabama, USA), 1992.
- [8] A. Hatcher, *Algebraic Topology*, Cambridge University Press, 2002.
- [9] J. Eckhoff, “Helly, Radon, and Carathéodory Type Theorems.” Ch. 2.1 in *Handbook of Convex Geometry* (Ed. P. M. Gruber and J. M. Wills). Amsterdam, Netherlands: North-Holland, pp. 389-448, 1993.
- [10] C.-F. Huang and Y.-C. Tseng, “The coverage problem in a wireless sensor network,” in *ACM Intl. Workshop on Wireless Sensor Networks and Applications*, pp. 115121, 2003.
- [11] A. Jadbabaie, “On geographic routing without location information,” in *Proc. IEEE Conf. on Decision & Control*, 2004.
- [12] T. Kaczynski, K. Mischaikow, and M. Mrozek, *Computational Homology*. Applied Mathematical Sciences 157, Springer-Verlag, 2004.
- [13] H. Koskinen, “On the coverage of a random sensor network in a bounded domain,” in *Proceedings of 16th ITC Specialist Seminar*, pp. 11-18, 2004.
- [14] X.-Y. Li, P.-J. Wan, and O. Frieder, “Coverage in wireless ad-hoc sensor networks” *IEEE Transaction on Computers*, Vol. 52, No. 6, pp. 753-763, 2003.
- [15] B. Liu and D. Towsley, “A study of the coverage of large-scale sensor networks,” in *IEEE International Conference on Mobile Ad-hoc and Sensor Systems*, 2004.
- [16] S. Meguerdichian, F. Koushanfar, M. Potkonjak, and M. Srivastava, “Coverage problems in wireless ad-hoc sensor network,” in *IEEE INFOCOM*, pp. 13801387, 2001.
- [17] A. Rao, S. Ratnasamy, C. Papadimitriou, S. Shenker, and I. Stoica, “Geographic routing without location information,” in *Proc. MobiCom*, 2003.
- [18] M. Smith and B. Freisleben, “Self-healing wireless ad hoc networks based on adaptive node mobility,” in *Proc. IFIP Conf. on Wireless and Optical Communications Networks*, 2004.
- [19] F. Xue and P. R. Kumar, “The number of neighbors needed for connectivity of wireless networks,” *Wireless Networks*, pp. 169-181, vol. 10, no. 2, March 2004.
- [20] H. Zhang and J. Hou, “Maintaining Coverage and Connectivity in Large Sensor Networks,” in *International Workshop on Theoretical and Algorithmic Aspects of Sensor, Ad hoc Wireless and Peer-to-Peer Networks*, Florida, Feb. 2004
- [21] A. Zomorodian and G. Carlsson, “Computing persistent homology,” in *Proc. 20th ACM Sympos. Comput. Geom.* pp. 346-356, 2004.
- [22] CHomP home page, <http://www.math.gatech.edu/~chomp/>
- [23] Plex home page, <http://math.stanford.edu/comptop/programs/plex/>